Hidden paleosols on a high-elevation Alpine plateau (NW Italy): Evidence for Lateglacial Nunatak?

Hidden paleosols on a high-elevation Alpine plateau (NW Italy): evidence for Lateglacial Nunatak?

Pintaldi E.[1], D'Amico M.[1,2], Colombo N.[1,2,3,*], Martinetto E.[3], Said-Pullicino D.[1], Giardino M.[3], Freppaz M.[1,2]

[1]Università degli Studi di Torino - DISAFA, Largo Paolo Braccini 2, 10095, Grugliasco (TO), Italy

[2]Università degli Studi di Torino, NATRISK, Research Centre on Natural Risks in Mountain and Hilly Environments, Largo Paolo Braccini 2, 10095, Grugliasco (TO), Italy

[3]Università degli Studi di Torino - DST, Via Valperga Caluso, 35, 10125 Torino (TO), Italy

*_Correspondence to_: nicola.colombo@unito.it (N. Colombo)

Abstract

Alpine soils can provide valuable paleo-environmental information, representing a powerful tool for paleoclimate reconstruction. However, since Pleistocene glaciations and erosion-related processes erased most of the pre-existing landforms and soils, reconstructing soil and landscape development in high-mountain areas can be a difficult task. In particular, a relevant lack of information exists on the transition between the Last Glacial Maximum (LGM ~21,000 yr BP) and the Holocene (~10,000 yr BP), with this climatic shift that plays a crucial role for environmental thresholds identification. The present study aims at reconstructing the history and origin of hidden paleosols inside periglacial blockstreams and blockfields on a high-elevation Alpine plateau (Stolenberg Plateau) above 3000 m a.s.l., in the Northwestern Italian Alps. The results indicate that these soils recorded the main warming climatic phases occurring from the end of the LGM until the beginning of Neoglacial (~4,000 yr BP). Our reconstructions, together with the high carbon stocks of these paleosols, suggest that during warming phases the environmental conditions on the Plateau were suitable for plant life and pedogenesis, already since 22,000-21,000 yr BP. These paleosols reasonably evidence the existence of a Lateglacial nunatak representing, to our knowledge, one of the first documented relict non-glacial

surfaces in the high-elevated European Alps. Thus, the Stolenberg Plateau provides important information about past climate and surface processes, suggesting new perspectives on the long-term landscape evolution of the high European Alps.

Keywords: ^{14}C dating, $\delta^{13}C$, blockstream/blockfield, paleoclimate, Umbrisol, relict surface

Introduction

High-mountain areas can preserve traces of dramatic climatic variations, representing unique geosites and “storytellers" about the past landscape dynamics (Favilli et al., 2008). However, reconstructing soil and landscape evolution in such areas can be a difficult task because Pleistocene glaciations and related processes erased most of the pre-existing landforms and soils, leading to the formation of a complex mosaic of Quaternary sediments and soils of different ages (Sartori et al., 2001). Nevertheless, on scattered stable surfaces preserved during Pleistocene glaciations, ancient soils can be locally preserved for long periods (D’Amico et al., 2016). These soils, apparently in contrast with Holocene soil forming conditions, represent paleosols (when buried) or relict soils (Ruellan, 1971) that constitute excellent pedo-signatures of different specific past climatic/environmental conditions.

Relict surfaces are recognizable as flat summits and plateaus perched high above the valley floors at different elevations, in which erosion and deposition processes were very limited (D’Amico et al., 2016), because of lateral migration of glacial masses (Carraro and Giardino, 2004). Those surfaces that were not affected by the passage of glaciers experienced extreme cold conditions, which induced strong frost-action processes (e.g., frost-shattering, frost sorting, frost heave, etc.) (Karte, 1983), leading to the formation of periglacial features such as blockfields, blockstreams, and tors (Goodfellow, 2007; Ballantyne, 2010). Because of their high stability on certain poorly weatherable materials (D’Amico et al., 2019), these Pleistocene relict periglacial landforms are considered key

indicators of ancient non-glacial surfaces (Goodfellow, 2007). Therefore, they have been used in paleoclimatic reconstructions, as their formation can be associated with specific past environmental conditions (e.g., Karte, 1983; Wilson, 2013; D'Amico et al., 2019). In particular, blockfields, which are usually associated with mountain summits and plateaus, have been used as paleo-indicators of nunataks (e.g., Ballantyne and Harris, 1994; Ballantyne, 1998, 2010) or non-erosive ice covers such as cold-based glaciers (e.g., Nesje et al., 1988; Kleman and Borgström, 1990; Hättestrand and Stroeven, 2002).

Nunataks (Dahl, 1987) are isolated hills or mountain peaks that projected above the ice shields and alpine-type icecap (Fairbridge, 1968). They have been proposed as possible biological refugia during glacial periods (Schönswetter et al., 2005; Goodfellow, 2007; Birks and Willis, 2008), serving as sources for the rapid reoccupation of the later deglaciated landscape (Fairbridge, 1968). While several studies have been focused on nunataks especially at high latitudes (e.g., Birks, 1994; McCarroll et al., 1995; Ballantyne et al., 1998), there is a paucity of works that have studied nunataks in the European Alps (Schönswetter et al., 2005; Carcaillet and Blarquez, 2017; Carcaillet et al., 2018), likely due to intrinsic difficulties in finding relict surfaces preserved from glaciations. Moreover, although many studies proposed paleoclimatic reconstruction in Alpine environments, they were mostly localized at elevation lower than 2200 m a.s.l. and in different climatic conditions (e.g., Kerschner and Ochs, 2008; Samartin et al., 2012a; Heiri et al., 2014). Furthermore, while the environmental conditions from the Oldest Dryas to the Holocene are relatively well documented (e.g., Samartin et al., 2012b; Cossart et al., 2012, Heiri et al., 2014), a substantial gap of paleoclimate data during the transition between Last Glacial Maximum (LGM) and the Early Lateglacial still exists in the Alps, despite the well reported beginning of deglaciation, which occurred no later than 22,000-18,000 yr BP (Ivy-Ochs et al., 2006a; Ivy-Ochs, 2015, Monegato et al., 2017; Seguinot et al., 2018).

Based on these considerations, the object of this work is the reconstruction of the history of a high-elevation Alpine plateau (Stolenberg Plateau), covered by periglacial features, located in the Northwestern Italian Alps at 3000 m a.s.l. More specifically, this work aims at investigating the age

and origin of soils discovered within blockstreams and blockfields (Pintaldi et al., 2021), through the application of I) plant remains investigation (carpological approach), II) plant fragments and soil ^{14}C dating, and III) soil $\delta^{13}C$ analysis. Moreover, based on the interpretation of the obtained results and literature data, the work aims at IV) reconstructing the possible paleoenvironmental evolution of this high-elevated periglacial landscape since the end of the LGM.

2. Materials and Methods

2.1 Study Area

The Stolenberg Plateau (3030 m a.s.l.) is located at the foot of the southern slope of Monte Rosa (4634 m a.s.l.), along the border between Valle d'Aosta and Piemonte regions, NW Italian Alps (Long-Term Ecological Research-LTER site Istituto Mosso, 45°52'42.87"N, 7°52'0.64"E) (Fig. 1, Supplementary material 1). The Plateau has a south-east orientation and covers a surface of ca. 1.35 ha, with a slope angle between 0° and 13°. Meteorological parameters of the study area (air temperature and total liquid precipitation) were recorded by the Bocchetta delle Pisse Automatic Weather Station (AWS) (2401 m a.s.l., managed by ARPA Piemonte), located ca. 2.5 km east of the study area (on the same slope). The temperatures at the Plateau were obtained using the standard lapse rate of 6 °C km^{-1}. The mean cumulative annual snowfall was recorded by the Col d'Olen AWS (2901 m a.s.l., managed by the Italian Army, Comando Truppe Alpine - Servizio Meteomont), located ca. 500 m south-east of the Plateau. The LTER area has a total annual precipitation of ca. 1300 ±270 mm (1997-2019) at 2400 m a.s.l., with a winter minimum and a late spring-summer maximum. The Plateau has a mean annual air temperature of –2.4 ±0.7 °C (1988-2019) and a mean summer (June, July, August) air temperature of 4.4 ±1.3 °C; July is the warmest month, with a mean air temperature of 5.2 ±2.7 °C. The mean annual liquid precipitation is ca. 358 ±86 mm (1997-2019) while the mean cumulative annual snowfall is ca. 800 ±143 cm, with a snow cover lasting for at least 8 months (2008-2019).

The Plateau is covered by a thick layer of stones of variable size (from decimetric to metric), well organized in autochthonous blockfields, blockstreams/sorted stripes, gelifluction lobes, tilted stones, and weakly developed sorted circles (Pintaldi et al., 2021). No glacial striations or roches moutonnées have been detected on the few highly fractured rock outcrops. The parent material is composed of gneiss and mica-schists (Monte Rosa nappe, Pennidic basement), and metabasites (Zermatt-Saas unit) (Tognetto et al., 2021). The vegetation cover, which is almost absent or confined to small patches, reaching no more than 5% of the Plateau surface, is composed of alpine species such as *Silene acaulis*, *Carex curvula, Salix herbacea* in the vegetated patches, while *Festuca halleri, Poa alpina, Ranunculus glacialis, Leucanthemopsis alpina, Cerastium uniflorum, Oxyria digyna* and a few other scattered species grow also in the stone-covered area. No relevant permafrost bodies have been detected in the site, even though some permafrost patches cannot be excluded (Pintaldi et al., 2021). The ground surface thermal regime monitoring (2019-2020) showed no significantly negative soil temperatures under the blockstreams (Supplementary material 2, Fig. S1,2). However, during the snow-free season, soil temperatures under these periglacial features were colder than in nearby snowbed soils covered by vegetation (Supplementary material 2, Fig. S3, Tab. S1).

2.2. Soil characteristics

In 2017, during operational activities for constructing a new cableway station on the Plateau, three soil trenches were opened in the construction area close to the protected geosite (soil profiles P1, P2, and P3 in Fig. 1), revealing surprisingly well-developed soils under the stony cover. These soils were characterized by dark and thick organic C-rich A horizons (Fig. 2,3,4), and were classified as Skeletic Umbrisol (Arenic, Turbic), according to IUSS Working Group WRB (2015). Soil texture was generally loamy sand or sandy loam, pH (measured in H_2O) values were extremely to moderately acidic and carbonates were absent. Total Organic Carbon (TOC) content reached maximum values of ca. 20 g kg^{-1} in the A horizons of profiles P1 and P2 and over 10 g kg^{-1} in profile P3; the soil C

stocks (up to ~ 5 kg m^{-2}) were comparable to vegetated or even forest soils, despite the extremely sparse vegetation cover (Pintaldi et al., 2021). Geophysical investigations indicated that these hidden soils were widespread on the Plateau. The detailed description of the soil profiles, as well as their physical and chemical properties, distribution and thickness, are reported in Pintaldi et al. (2021).

2.3. Plant remains analysis

The presence of few plant fragments mixed within the soil material was observed within soil samples collected from the umbric A horizons in the soil profiles. In order to isolate and identify the plant fragments within soil matrix, to reconstruct the possible past vegetation of the Plateau, a carpological approach was adopted, starting from the assumption that plant material contained in paleosols may preserve the main features of soil "seed banks" (Ter Heerdt et al., 1996). Furthermore, the investigation was applied on two additional soil samples collected deep inside a soil-filled rock wedge (a vertical fracture in the substrate filled with vertically stratified soil materials, likely formed by freeze-thaw action), at 3 m depth (Fig. 5) along the southern border of the plateau (site “Wedge” in Fig. 1). We used the standard method (Supplementary material 3) for extraction of seeds and fruits from deep time sediments (e.g., Martinetto, 2009; Martinetto and Vassio, 2010), because recent experiences (Bertolotto et al., 2012) on a few soils showed that this was effective.

2.4. Plant fragments and soil ^{14}C dating

Radiocarbon dating (^{14}C) was performed on six plant fragment samples, accurately selected after the carpological investigation: five samples, consisting of recognizable but fossil-resembling plant fragments (dark coloured, mineral coatings), were obtained from soil samples collected in the umbric A horizons (usually in the 0-10 cm layer); one sample, consisting of unrecognizable plant fragments (strongly decomposed), derived from soil samples collected in the soil wedge at 3 m depth. Furthermore, ^{14}C radiocarbon dating was performed on ten soil samples, nine of which selected from

soil profiles: two from profile P1 (1,2), four from P2 (7,8,9,9bis) and three from P3 (2,3,5) (Fig. 1); one sample was collected in the only fully vegetated patch of the plateau (P4), at 10-20 cm depth (A horizon) (Fig. 1). The radiocarbon dating was performed at CEDAD, the Centre for Applied Physics, Dating and Diagnostics, Department of Mathematics and Physics "Ennio de Giorgi" - University of Salento, Lecce, Italy, using radiocarbon accelerator mass spectrometry (AMS) analysis (Calcagnile et al., 2005) and the standard preparation methods (D'Elia et al., 2004). Radiocarbon dates of soil samples were calibrated in calendar age by using the software OxCal Ver. 3.10 (Supplementary material, Figs. S4-S14), based on atmospheric data (Reimer et al., 2013). Further methodological details can be found in Supplementary material 4.

2.5 Soil $\delta^{13}C$ stable isotope signature

To verify the typical $\delta^{13}C$ signature of present-day vegetated soils in the study area, which clearly reflects the existing vegetation (Meyer et al., 2014), soil samples were collected from the A horizons of five vegetated permanent study areas at slightly lower elevation in the LTER site (2750-2900 m a.s.l., Supplementary material 5). Moreover, the analysis was performed on fourteen selected soil samples (A horizons) from the Plateau (Supplementary material 5). Samples were air-dried, sieved to 2 mm and checked using stereomicroscope to eventually remove macro-contaminants. Then samples were ground and sieved to 0.5 mm. The $\delta^{13}C$ signature of total organic carbon (due to the absence of carbonates) was directly determined using an Isoprime 100 continuous flow stable isotope mass spectrometer coupled to a Vario Isotope Select elemental analyzer (EA-IRMS; Elementar Analysensysteme GmbH, Hanau, Germany) and expressed in parts per thousand (‰) relative to the international standard Vienna Pee Dee Belemnite (VPDB) (further methodological details in Supplementary material 5). Significant differences (p-value < 0.05) in $\delta^{13}C$ values between present-day vegetated soils and soils under periglacial features were evaluated through one-way analysis of

variance (ANOVA) combined with Tukey HSD test. Statistical analyses were performed using R software, v. 3.6.0 (R Core Team, 2019).

3. Results

3.1. Plant remains and ^{14}C dating

The quantity of plant fragments found in the soils was very scarce, representing a negligible fraction compared to the soil matrix. However, they were composed of remains with definite morphologies, including cm-sized leaves (consisting mainly of well-preserved and recognizable specimens of *Salix herbacea, Cerastium uniflorum* and *Poaceae* sp.) and mm-sized fruits and seeds, which have been mostly identified as belonging to taxa growing today in surrounding snowbed areas and in the small vegetated patch on the Plateau (Tab. 1, Fig. 1). Only in sample F, which was collected inside the wedge (Fig. 5), the degree of decomposition was much higher, so that the morphology of larger plant fragments was vague and not recognizable. Only a few tiny fruits and seeds still had diagnostic morphologies and allowed the identification of some plant taxa (Tab. 1) Concerning radiocarbon dating, the plant fragment samples were all modern (after 1950 AD, Tab. 2), except the strongly decomposed sample F, which was dated back to 1,824-1,594 yr cal. BP.

3.2. Soil Organic Matter ^{14}C dating and $\delta^{13}C$ signature

Unlike plant fragments, the results from AMS on soil samples revealed a wide range of ages, covering several thousands of years and different well-distinct climatic periods, between ca. 22,000-21,000 yr and 4,400-4,100 yr cal. BP (Tab. 2). All radiocarbon dates were rounded and here presented as calibrated radiocarbon ages (yr cal. BP = years before 1950 A.D.). In P1 the age of soil samples was related with depth, in fact the oldest samples P1-1, dated between 8,782 and 8,412 yr cal. BP, was located close to the lower boundary of the umbric A horizon, while the youngest one (P1-2), dated between 5,735 and 5,589 yr cal. BP, was located close to the surface stones-soil interface (Fig.

2). In P2 the age of the samples was not related to depth: the oldest sample P2-9, dated between 17,584-16,985 and 18,148-17,719 (P2-9bis) yr cal. BP (values obtained from two independent and blind datings performed in different moments), was located close to the surface stones-soil interface, while the stable organic C in C-rich cryoturbated patches (P2-7), located close to the lower boundary of the umbric A horizon, was much younger (6,506-6,306 yr cal. BP) (Fig. 3); the central and rather homogeneous part of the A horizon (P2-8) dates back to 8,561-8,300 yr cal BP. In P3 the age of the samples was not related to depth as well: the oldest samples P3-2 and P3-3, dating back to 18,921-18,518 and 22,145-21,427 yr cal. BP respectively, were taken from homogeneous materials in the central part of the umbric horizon, while a younger radiocarbon age was obtained in the deeper part of the A horizon, close to the lower boundary (sample P3-5), dating back to 13,306-13,076 yr cal. BP (Fig. 4). The youngest soil sample, P4, taken from the A horizon in the currently fully vegetated patch, was dated between 4,360 and 4,090 yr cal. BP (Tab. 2).

The $\delta^{13}C$ signature of present-day vegetated soils provided by EA-IRMS ranged between -23.3 (Site 1) and -25.7 ‰ (Site 3), with a mean value of -24.2 ‰ (+/-1.1) (Tab. 3). The $\delta^{13}C$ of soil samples from the plateau showed very similar values, ranging between -23.5 (P3-3) and -24.7 ‰ (P1-1), with a mean of -24.1 ‰ (+/- 0.4), while the soil sample collected from the vegetated patch (P4) had a slightly greater value of $\delta^{13}C$ of -22.7 ‰ (Tab. 3). No significant differences were detected between present-day vegetated soils and soils under periglacial features (Supplementary material, Fig. S15).

4. Discussion

4.1 Plant fragments ^{14}C dating

The plant fragment samples were generally modern (Tab. 2), except sample F, which was dated between 1,824 and 1,594 yr BP, corresponding therefore to the small warm phase occurred during the Roman time (Mercalli, 2004). The strong difference in age between sample F and the other samples was already reflected in the different degree of decomposition, as the larger plant fragments

226 in sample F were not recognizable. This sample, collected at ca. 3 m depth below the present-day
227 surface inside a rock wedge, evidenced strongly active periglacial processes, sufficient to activate the
228 rock wedge and thus its filling by surface soil material in the following centuries. This indicates that
229 cryoturbation processes acted across millennia, strongly mixing plant fragments within the soil
230 matrix, until they became unrecognizable. The presence of modern plant fragments within the soil
231 matrix, although very scarce, can be explained mainly by the aeolian transport from the surrounding
232 vegetated surfaces. The plant material could have been trapped by the stone layer and moved towards
233 the soil surface through the large spaces between the rocks. Alternatively, a small input from the
234 sporadically occurring vegetation growing within the stones may have contributed.
235

236 ## 4.2 Soil ^{14}C dating

237 Radiocarbon dating of soils and sediments can be problematic due to the presence of pre-aged
238 carbon (e.g., Lowe and Walker, 2000; Pessenda et al., 2001; Thorn et al., 2009) or fresh/allochthonous
239 organic matter (Wang et al., 1996; Tonneijck et al., 2006). Therefore, terrestrial plant macrofossils
240 have been considered the most reliable material for ^{14}C dating (Lowe and Walker, 2000; Hatté et al.,
241 2001). However, the fossil record of the Alpine flora is generally scarce due to the lack of conditions
242 suitable for the accumulation of macro-remains at the highest elevations (Lang, 1994). If materials
243 such as charcoal, wood, or other plant macrofossils (Muhs et al., 2003) are lacking, dating of soils or
244 sediments is generally accepted (Wang et al., 2014), especially in specific sites and under certain
245 conditions (Lowe and Walker, 2000). Thus, the interpretation of ^{14}C dates must be adapted to the
246 specific soil ecosystem under study (Tonneijck et al., 2006).
247 Differently from plant samples, datings of the soil samples collected from the Plateau covered an
248 extended time interval, involving both Pleistocene and Holocene epochs. If some kind of very old-
249 aged material (i.e. from LGM or even older) was deposited on the Plateau surface, it should have
250 been deposited also on the nearby glacier surfaces. However, similar old-aged organic materials have

never been detected in the well-studied Monte Rosa glaciers (Jenk et al., 2009; Thevenon et al., 2009). Currently, the oldest date obtained from an ice core, collected at ~80 m depth on the nearby Colle Gnifetti, was around 15,000 yr (Jenk et al., 2009). In the European Alps, on glacier surfaces, the most important source for the deposition of already aged organic materials is soil dust (Hoffman, 2016), a large part of which is originated from Saharan dust storm (e.g., Wagenbach and Geis, 1989; Wagenbach et al., 1996; Hoffman, 2016). The age of organic matter in these atmospheric depositions range between 1,000 and 5,000 yr (Eglinton et al., 2002; Jenk et al., 2006), with a mean of ca. 2,500 (Hoffman, 2016). Finally, the contribution of anthropogenic emissions was also considered as a possible cause for the aging of samples (Jenk et al., 2006), the so-called Suess effect (Suess, 1955). However, this effect is generally negligible on the samples older than 2,000-5,000 yr BP (Graven et al., 2015; Köhler, 2016). Therefore, most of our samples, especially the oldest ones, were out of the range of influence of the Suess effect.

Based on the previous considerations, our soil samples cannot therefore be influenced by other than local organic carbon sources (i.e. vegetation grown during warming phases). Furthermore, the soil texture of the paleosols at the Stolenberg Plateau was loamy sand or sandy loam and no differences were found among profiles and between surface and deep samples (Pintaldi et al., 2021), thus rejecting also the hypothesis of a Loess deposition, which is otherwise mainly composed of silt-sized material dominated by quartz (Smalley et al., 2006), but could also include organic matter.

These soils could have experienced several different climatic conditions, retaining information about past climates, ranging from the end of the LGM (Ivy-Ochs, 2015) to the beginning of the Neoglacial (Orombelli et al., 2005). All the detected ages matched exactly and exclusively with the main warming phases/interstadials occurring from the LGM until the transition between the Holocene Climatic Optimum (HCO) and the Neoglacial (Deline and Orombelli, 2005; Ivy-Ochs et al., 2009), whereas no soil samples from cold phases/stadials were detected (further details in chapter 5).

The surface position of the oldest samples and the general inversion of the typical age-depth relationship can be explained by the strong cryoturbation processes occurring on the Plateau,

especially during the cold climatic phases. Indeed, cryoturbation processes mix and displace soil horizons (Bockheim and Tarnocai, 1998; Pintaldi et al., 2016), redistributing organic matter (e.g., van Vliet-Lanoë et al., 1998; Hormes et al., 2004; Bockheim, 2007). Furthermore, other works reported inverted soil age-depth relationship (e.g., Carcaillet et al., 2001; Favilli et al., 2008; Egli et al., 2009; Serra et al., 2020), as the young and contemporary carbon can be transported by soil turbation processes, such as cryoturbation and bioturbation, thus contributing to the rejuvenation of the subsoil (Scharpenseel and Becker-Heidmann, 1992; Rumpel et al., 2002; Favilli et al., 2008). Besides the well-developed periglacial features, cryoturbation processes were also evidenced by the internal soil morphology, which showed inclusions of surface A-horizon materials at depth, as well as strong convolutions and block displacement above wedges (Pintaldi et al., 2021).

Remarkably, ages similar to the ones of our oldest samples have never been detected in soils at such high-elevated ecosystems in the European Alps. For instance, Baroni and Orombelli (1996) found a Cambisol with buried A horizons at Tisa Pass (3200 m a.s.l.), but with a radiocarbon age of around 6,400-6300 yr BP , while Orombelli (1998) obtained an age up to ca. 9,000 yr BP (2500 m a.s.l.) for the Rutor Peat Bog. As reported by Ivy-Ochs et al. (2008), the oldest date yet obtained for an ice-free Swiss foreland is 17,000-18,000 yr, although it is a minimum age, because pinpoint the timing during this period, using radiocarbon age, remains difficult due to the lack of organic material (Kerschner and Ivy-Ochs, 2008), which is rare and often reworked (Ivy-Ochs et al., 2008). Glacier basal sediments at the Jamtalferner and Stubai glaciers (Austria) had ages around 17,000 and 22,000 yr BP, respectively (Hoffman, 2016). Furthermore, although at lower elevation (2100 m a.s.l.), Favilli et al. (2008, 2009) obtained comparable ages (17,000-18,000 yr BP) for an Entic Podzol, in the alpine belt in NE Italy. Other comparable radiocarbon ages (~21,000 yr BP) were reported by Carcaillet and Blarquez (2017) for a tree refugium at ~2200 m a.s.l., in the Western Alps.

4.3 Soil $\delta^{13}C$ signature

The soil $\delta^{13}C$ signatures are frequently used to reconstruct plant community history and the sources of soil organic carbon (Bai et al., 2012). As plant residues enter the soils, their $\delta^{13}C$ values may be modified slightly from their original values by isotope fractionation associated to preferential C mineralization (Bai et al., 2012). The overall $\delta^{13}C$ signature of present-day vegetated soils obtained by the stable isotope analysis, was comparable to those reported for soils and alpine vegetation in high-elevation ecosystems (Bird et al., 1994; Körner et al., 1991, 2016; Körner, 2003). The $\delta^{13}C$ signatures of soils under periglacial features corresponded very well with those of present-day vegetated soil (Tab. 3), thus indicating that the soil organic carbon probably originated from alpine plants with the same isotopic signature of present-day vegetation. Furthermore, studies conducted by Colombo et al. (2020) on a nearby rock glacier at ~2700 m a.s.l., indicated $\delta^{13}C$ values of surrounding vegetated soils (-24.5 ‰) very similar to those of the Plateau, while the $\delta^{13}C$ signature of the active rock glacier soil, characterized by cold ground thermal regimes, coarse debris cover, and extremely reduced plant cover, increased considerably (ca. -18 ‰). Thus, the overall correspondence of the $\delta^{13}C$ signatures between present-day vegetated soils and paleosols under periglacial features suggested a common origin of the soil organic carbon from very similar alpine flora.

5. Historical and paleoenvironmental setting

In Fig. 6 we propose a conceptual model reporting a tentative paleoenvironmental reconstruction of the Stolenberg Plateau. Despite uncertainties, we believe that it may facilitate the interpretation of our data and also the generation (and testing) of the different hypotheses, as it includes and coordinates the different evidences we collected.

The LGM (Fig. 6A1-B1) ended around 22,000-19,000 yr BP (Ivy-Ochs et al., 2006a; Gianotti et al., 2015; Ivy-Ochs, 2015; Monegato et al. 2017), during which transection glaciers, flowing into valley systems, characterized the Western European Alps (Kelly et al., 2004). The mean air temperature was ~12 °C lower than present day in the European Alps (Peyron et al., 1998; Becker et

al., 2016) and the mean July air temperature was likely around -4/5 °C on the Plateau (cf. Renssen et al., 2009; Samartin et al., 2012a,b; Heiri et al., 2015). Considering the lack of soil samples older than ca. 22,000 yr and the inferred cold conditions during LGM, together with the strongly weathered, autochthonous soil and stone materials, we can hypothesize the presence of a barren cryoturbated surface or of a small cold-based "ice cap" covering the Plateau (Fig. 6A1-B1).

Our oldest ^{14}C datings (P3-2, P3-3, P2-9, and P2-9bis) span from 22,000 to 17,000 yr BP, falling exactly during a period of massive downwasting of transection glaciers (Early Lateglacial Ice Decay-ELID) (e.g., Ravazzi, 2005; Ivy-Ochs et al., 2006a, 2008; Monegato et al., 2007; Reitner, 2007; Wirsig et al., 2016). Glacial shrinking also occurred at high elevations (Dielfolder and Hetzel, 2014), with some mountain peaks, around 2300-2600 m a.s.l., protruding out of the ice surface (Wirsig et al., 2016). The ELID occurred on both sides of the Alps due to significant rise in air temperatures (e.g., Huber et al., 2010; Schmidt et al., 2012; Samartin et al., 2012a,b). Assuming a pronounced climate continentality (Jost-Stauffer et al., 2001; Ivy-Ochs et al., 2009), summer air temperatures were likely similar to the ones inferred for the Bølling-Allerød interstadial (e.g., Huber et al., 2010; Samartin et al., 2012a,b; Schmidt et al., 1998, 2012). In addition, soil surface temperatures in alpine environments during summer are generally 2-4 °C above the air temperatures (Scherrer and Körner, 2010), indicating that life conditions of alpine organisms growing on the soil surface can be strongly decoupled from conditions in the free atmosphere, particularly on south oriented surfaces like the Plateau (e.g., Scherrer and Körner, 2010). Our ancillary measurements confirmed that the mean 10 cm depth soil temperature during summer was ~3 °C warmer than air temperature on the Plateau (vegetated patch GST2), while at slightly lower elevation soil temperatures was 1-3 °C warmer (Supplementary material 2, Tab. S2). Therefore, the Stolenberg Plateau was likely ice-free since ~22,000-21,000 yr BP, i.e. the (micro)climatic conditions were probably suitable for pedogenesis and growth of some vegetation (Fig. 6A2,3-B2,3).

No radiocarbon ages were detected in our soils between ~17,000 yr BP and ~14,700 yr BP, which was a period (Gschnitz stadial or Oldest Dryas; Walker et al., 1999; Ivy-Ochs et al., 2006b, 2008)

353 characterized by a decrease of both temperatures and precipitations, with values 8.5-10 °C and 25-50
354 % lower than the respective modern values (Ivy-Ochs et al., 2006a,b; Kerschner and Ivy-Ochs, 2008;
355 Ivy-Ochs, 2015). These cold climatic conditions allowed a readvance of mountain glaciers (Kerschner
356 et al., 2002; Ivy-Ochs et al., 2006a,b, 2008). Thus, it is probable that the environmental conditions on
357 the Plateau were not suitable to sustain plant life and pedogenesis, while they favored strong frost-
358 action processes which led to the activation of periglacial features (Goodfellow, 2007; Ballantyne,
359 2010) (Fig. 6A4-B4).
360 The age of the P3-5 sample, dated between 13,306 and 13,076 yr cal. BP, matched perfectly with
361 a warm period occurred between ~14,700 and 12,900 yr BP, corresponding to the Bølling-Allerød
362 interstadial (Rasmussen et al., 2006; Ivy-Ochs et al., 2008; Dielfolder and Hetzel, 2014). A strong
363 rise in the mean annual air temperatures was inferred (ca. 3 °C), with respect to the Oldest Dryas,
364 causing the melting of valley glaciers (e.g., Ravazzi, 2005; Vescovi et al., 2007; Dielfolder and
365 Hetzel, 2014). Other studies indicated even greater rises in temperature, ~3-4 °C (Larocque-Tobler et
366 al., 2010) and ~5 °C (Renssen and Isarin, 2001). The mean July temperature at the Plateau, during
367 this period, may have been higher than 3 °C (cf., Heiri and Millet, 2005; Samartin et al., 2012a,b;
368 Dielfolder and Hetzel, 2014). Thus, the summer climate could have been suitable again for
369 pedogenesis and plant life (Fig. 6A5-B5).
370 After the Bølling-Allerød, a general worsening of climate conditions occurred, leading to another
371 cold phase, the Younger Dryas, also called Egesen Stadial (Ivy-Ochs et al., 2006b, 2008), which
372 lasted until 11,700 yr BP. The summer temperatures were 3.5-4 °C lower, while precipitation was
373 reduced by 10 to 30% compared to modern values (Kerschner et al., 2000, Kerschner and Ivy-Ochs,
374 2008). Again, on the Plateau, no soil radiocarbon ages were detected from this cold period, as the
375 environmental conditions likely favored frost-action processes rather than pedogenesis, probably
376 leading to a new expansion of periglacial features (Fig 6A6-B6).
377 The ages of four soil samples (P1-1, P1-2, P2-7, and P2-8) span from 8,700 to 5,700 yr BP,
378 corresponding to the warm Holocene Climatic Optimum (HCO), occurred between 10,000 and 5,000

yr BP (Mercalli, 2004; Orombelli, 2011). In this period a ~3-4 °C temperature increase was estimated with respect to the Younger Dryas (e.g., Tinner and Kaltenrieder, 2005; Ilyashuk et al., 2009; Larocque-Tobler et al., 2010; Samartin et al., 2012b). Glaciers were probably smaller than present day during the height of the HCO (e.g., Ivy-Ochs et al., 2009; Orombelli, 2011; Grämiger et al., 2018; Bohleber et al., 2020). Mean air temperature was up to 1-2 °C warmer with respect to the present-day values in the European Alps (e.g., Grove, 1988; Nesje and Dahl, 1993; Antonioli et al., 2000; Ivy-Ochs et al., 2009) and the inferred July temperature at the Plateau may have reached values around 6-7 °C (or even more) (cf. Ilyashuk et al., 2009; Samartin et al., 2012b), therefore above present-day values (cf., Birks and Willis, 2008; Ilyashuk et al., 2009; Samartin et al., 2012b). This likely led to conditions suitable for plant life (Fig. 5A7-B7).

The age of our youngest sample (P4), dated 4,360-4,090 yr BP, corresponded with a period of climate stability or slight cooling encompassed between 5,000 and 4,000 yr BP, after which a strong decrease in temperature was estimated (Heiri et al., 2015), which led to Alpine glacier expansion from 3,300 yr BP (Ivy-Ochs et al., 2009); this period has been called Neoglacial (Deline and Orombelli, 2005; Orombelli, 2005). After 3,300 yr BP, colder climatic conditions caused prolonged and frequent glacier advances, leading finally to the Little Ice Age (LIA, 1300-1850 A.D.) (Ivy-Ochs et al., 2009). During this last and prolonged cold phase, no soil radiocarbon ages were detected at the Plateau, apart from highly weathered plant fragments collected deep inside the rock wedge. The frost action likely prevailed, causing the final expansion of the periglacial features and the complete covering of the Plateau (Fig. 5A8-B8), while few plants could thrive without being able to leave measurable amounts of organic matter in the soil horizons.

6. Nunataks: yes or no?

The nunatak theory hypothesizes that unglaciated reliefs in glacial and periglacial areas acted as a refugium for isolated colonies of microorganisms, plants, and animals which survived the rigorous

404 condition of the last glacial times for a few thousand years (Fairbridge, 1968; Dahl, 1987). These
405 nunataks could have served as center for the recolonization of the later deglaciated landscape
406 (Fairbridge, 1968). However, clear evidence for in situ survival of alpine floras on nunataks in the
407 Alps during the last ice age are rather limited (e.g., Stehlik, 2002; Schönswetter et al., 2005; Carcaillet
408 and Blarquez, 2017; Carcaillet et al., 2018) and subjected to a heated debate (e.g., Gugerli and
409 Holderegger, 2001; Carcaillet and Blarquez, 2019; Finsinger et al., 2019). The existence and
410 identification of such refugia during glacial or interglacial stages has been a topic of active research
411 for decades (Hampe et al., 2013). The recolonization of the Alps would have started not only from
412 peripheral refugia, but also from areas within the ice sheet (Schönswetter et al., 2005), where isolated
413 nunataks could have been sources and targets as well of species immigration and establishment (Paus
414 et al., 2006). Indeed, barren substrate or saprolite (Goodfellow, 2007), exposed just after glacier
415 retreat (Fig. 6A2-B2), could become targets of autotrophic organisms (e.g., algae, mosses, lichens,
416 higher plants), starting the process of primary succession (Bardgett et al., 2007). Thus, nunataks may
417 have been indeed inhabited for several thousand years during the last glaciation (Gugerli and
418 Holderegger, 2001), before the surrounding lowlands became deglaciated and invaded by organisms
419 in the early Holocene. Remarkably, the Plateau location matched exactly with an area assumed to be
420 a potential refugia for the survival of high-elevation plants on ice-free mountain tops within the
421 strongly glaciated central parts of the Alps, particularly among the north of the Aosta Valley (NW-
422 Italy) and south Valais, and within the mountain ranges of Monte Rosa (Stehlik, 2002; Schönswetter
423 et al., 2005; Kosiński et al., 2019).

424 Based on the results reported here and the presence of strong geomorphological evidences (i.e.
425 periglacial features such as blockstreams/blockfields), as well as the overall specific morphology,
426 aspect and position, the Stolenberg Plateau is thought to represent a Lateglacial Alpine Nunatak, on
427 which specific pedoclimatic conditions could have been suitable for alpine plant life already since
428 22,000-21,000 yr BP. As sometimes observed at high elevation at present day (e.g. *Saxifraga*
429 *oppositifolia* growing at 4500 m a.s.l. near the summit of Dom in Switzerland, Körner, 2011),

soil/substrate temperatures can be increased by solar surface warming in specific protected sites. This is particularly true where adiabatic winds, topography, local rock warming effect (Carturan et al., 2013), long-wave radiation from nearby rocky walls (i.e., the Mt. Stolenberg rock wall), and mass elevation effect (e.g. Monte Rosa Massif) (Samartin et al., 2012a), favor specific and stable microclimate features (e.g., Stewart and Lister, 2001), allowing the formation of the nunatak conditions.

6. Conclusion

In the severe periglacial environment of the Stolenberg Plateau, at 3030 m a.s.l., thick and well-developed Umbrisol were detected inside periglacial features (blockstreams/blockfields). As previously reported in Pintaldi et al (2021), these soils, despite the large stony cover and the scattered vegetation, showed carbon stocks comparable to alpine tundra or even forest soils. Radiocarbon dating and soil $\delta^{13}C$ signatures indicated that these hidden soils were paleosols that recorded exclusively the main warming phases occurring since the end of LGM until the beginning of Neoglacial. This finding suggests that the environmental conditions on the Plateau were suitable for alpine plant life and pedogenesis, already since the end of LGM. Our results, coupled with the inferred paleoclimate reconstruction, indicate that the Stolenberg Plateau can be considered a direct evidence of a Lateglacial Alpine Nunatak, representing therefore a valuable natural and historical archive for unravelling the post-LGM history of the high-elevation landscape of the European Alps.

Acknowledgments

This study was supported by European Regional Development Fund in Interreg Alpine Space project Links4Soils (ASP399): Caring for Soil-Where Our Roots Grow (http://www.alpinespace.eu/projects/links4soils/en/the-project). Many thanks to Monterosa Ski Resort (Monterosa 2000 and Monterosa SpA project stakeholders) for providing logistical support.

References

Antonioli, F., Baroni, C., Camuffo, D., et al., 2000. Le fluttuazioni del clima nel corso dell'Olocene: stato dell'arte. Il Quaternario 13(1/2), 95–128.

Bai, E., Boutton, T.W., Liu, F., et al., 2012. Spatial variation of soil $\delta^{13}C$ and its relation to carbon input and soil texture in a subtropical lowland woodland. Soil Biol. Biochem. 44(1), 102–112. https://doi.org/10.1016/j.soilbio.2011.09.013

Ballantyne, C.K., 1998. Age and significance of mountain-top detritus. Permafr. Periglac. Process. 9, 327–345. https://doi.org/10.1002/(SICI)1099-1530(199810/12)9:4<327::AID-PPP298>3.0.CO;2-9

Ballantyne, C.K., 2010. A general model of autochthonous blockfield evolution. Permafr. Periglac. Process. 21, 289–300. https://doi.org/10.1002/ppp.700

Ballantyne, C.K., Harris, C., 1994. The Periglaciation of Great Britain. Cambridge University Press, Cambridge, U.K.

Bardgett, R.D., Richter, A., Bol, R., et al., 2007. Heterotrophic microbial communities use ancient carbon following glacial retreat. Biol. Lett. 3, 487–490. https://doi.org/10.1098/rsbl.2007.0242

Baroni, C., Orombelli, G., 1996. The Alpine "Iceman" and Holocene Climatic Change. Quat. Res. 46, 78–83. https://doi.org/10.1006/qres.1996.0046

Becker, P., Seguinot, J., Jouvet, G., et al., 2016. Last Glacial Maximum precipitation pattern in the Alps inferred from glacier modelling. Geogr. Helv. 71, 173–187. https://doi.org/10.5194/gh-71-173-2016

Bertolotto, G., Martinetto, E., Vassio, E., 2012. Applicazioni paleobotaniche dello studio di resti carpologici in suoli e depositi fluviali attuali del Piemonte, con particolare riferimento alle Cyperaceae. Inf. Bot. Ital. 44 (2), 72–74.

Bird, M.I., Haberle, S.G., Chivas, A.R., 1994. Effect of altitude on the carbon-isotope composition of forest and grassland soils from Papua New Guinea. Glob. Biogeochem. Cycles 8(1), 13–22.

Birks, H.H., 1994. Plant macrofossils and the nunatak theory of per-glacial survival. Dissertationes botanicae 234, 129–143.

Birks, H.J.B., Willis, K.J., 2008. Alpines, trees, and refugia in Europe. Plant Ecol. & Divers. 1, 147–160. https://doi.org/10.1080/17550870802349146

Bockheim, J.G., 2007. Importance of Cryoturbation in Redistributing Organic Carbon in Permafrost-Affected Soils. Soil Sci. Soc. Am. J. 71, 1335. https://doi.org/10.2136/sssaj2006.0414N

Bockheim, J.G., Tarnocai, C., 1998. Recognition of cryoturbation for classifying permafrost-affected soils. Geoderma 81, 281–293.

Bohleber, P., Schwikowski, M., Stocker-Waldhuber, M., et al., 2020. New glacier evidence for ice-free summits during the life of the Tyrolean Iceman. Scientific Rep. 10(1), 1–10. https://doi.org/10.1038/s41598-020-77518-9

Calcagnile, L., Quarta, G., D'Elia, M., 2005. High-resolution accelerator-based mass spectrometry: precision, accuracy and background. Applied Radiation and Isotopes 62(4), 623–629. https://doi.org/10.1016/j.apradiso.2004.08.047

Carcaillet, C., 2001. Soil particles reworking evidences by AMS ^{14}C dating of charcoal. Comptes Rendus de l'Académie des Sciences Paris, Série Earth and Planetary Sciences 332, 21-28. DOI: 10.1016/S1251-8050(00)01485-3

Carcaillet, C., Blarquez, O., 2017. Fire ecology of a tree glacial refugium on a nunatak with a view on Alpine glaciers. New Phytol. 216, 1281–1290. https://doi.org/10.1111/nph.14721

Carcaillet, C., Latil, J.-L., Abou, S., Ali, A., Ghaleb, B., Magnin,F., Roiron, P., and Aubert, S., 2018. Keep your feet warm? A cryptic refugium of trees linked to a geothermal spring in an ocean of glaciers, Glob. Change Biol., 24, 2476–2487. https://doi.org/10.1111/gcb.14067

Carcaillet, C., Blarquez, O., 2019. Glacial refugia in the south-western Alps? New Phytol. 222(2), 663–667. https://doi.org/10.1111/nph.15673

505 Carraro, F., Giardino, M., 2004. Quaternary glaciations in the western Italian Alps - a review.
506 Developments in Quaternary Science 2(1), 201–208. https://doi.org/10.1016/S1571-
507 0866(04)80071-X
508 Carturan, L., Baroni, C., Becker, M., et al., 2013. Decay of a long-term monitored glacier: Careser
509 Glacier (Ortles-Cevedale, European Alps). The Cryosphere 7, 1819–1838.
510 https://doi.org/10.5194/tc-7-1819-2013, 2013.
511 Colombo, N., Ferronato, C., Antisari, L.V., et al., 2020. A rock-glacier–pond system (NW Italian
512 Alps): Soil and sediment properties, geochemistry, and trace-metal bioavailability. Catena 194,
513 104700. https://doi.org/10.1016/j.catena.2020.104700
514 Cossart, E, Fort M, Bourles D, Braucher R, Siame L. 2012. Deglaciation pattern during the
515 Lateglacial/Holocene transition in the southern French Alps. Chronological data and
516 geographical reconstruction from the Claree Valley (upper Durance catchment, southeastern
517 France). Palaeogeography Palaeoclimatology Palaeoecology 315-316: 109-123.
518 doi:10.1016/j.palaeo.2011.11.017
519 D'Amico, M.E., Catoni, M., Terribile, F., et al., 2016. Contrasting environmental memories in relict
520 soils on different parent rocks in the south-western Italian Alps. Quat. Int. 418, 61–74.
521 https://doi.org/10.1016/j.quaint.2015.10.061
522 D'Amico, M.E., Pintaldi, E., Catoni, M., et al., 2019. Pleistocene periglacial imprinting on
523 polygenetic soils and paleosols in the SW Italian Alps. Catena 174, 269–284.
524 https://doi.org/10.1016/j.catena.2018.11.019
525 Dahl, E., 1987. The nunatak theory reconsidered. Ecol. Bull. 77–94.
526 https://www.jstor.org/stable/20112974
527 D' Elia, M., Calcagnile, L., Quarta, G., et al., 2004. Sample preparation and blank values at the AMS
528 radiocarbon facility of the University of Lecce. Nuclear Instruments and Methods in Physics
529 Research Section B: Beam Interactions with Materials and Atoms 223, 278–283.
530 https://doi.org/10.1016/j.nimb.2004.04.056

Deline, P., Orombelli, G., 2005. Glacier fluctuations in the western Alps during the Neoglacial, as indicated by the Miage morainic amphitheatre (Mont Blanc massif, Italy). Boreas 34(4), 456–467. https://doi.org/10.1111/j.1502-3885.2005.tb01444.x

Dielfolder, A., Hetzel, R., 2014. The deglaciation history of the Simplon region (southern Swiss Alps) constrained by ^{10}Be exposure dating of ice-molded bedrock surfaces. Quat. Sci. Rev. 84, 26–38. https://doi.org/10.1016/j.quascirev.2013.11.008

Egli, M., Sartori, G., Mirabella, A., et al., 2009. Effect of north and south exposure on organic matter in high Alpine soils. Geoderma 149(1-2), 124–136. https://doi.org/10.1016/j.geoderma.2008.11.027

Eglinton, T. I., Eglinton, G., Dupont, L., et al., 2002. Composition, age, and provenance of organic matter in NW African dust over the Atlantic Ocean. Geochemistry, Geophysics, Geosystems, 3(8), 1–27. https://doi.org/10.1029/2001GC000269

Fairbridge, R.W., 1968. Glacial refuges (nunatak theory). In: Geomorphology. Encyclopedia of Earth Science. Springer, Berlin, Heidelberg.

Favilli, F., Egli, M., Cherubini, P., et al., 2008. Comparison of different methods of obtaining a resilient organic matter fraction in Alpine soils. Geoderma 145, 355–369. https://doi.org/10.1016/j.geoderma.2008.04.002

Favilli, F., Egli, M., Brandova, D., et al., 2009. Combined use of relative and absolute dating techniques for detecting signals of Alpine landscape evolution during the late Pleistocene and early Holocene. Geomorphol. 112, 48–66. https://doi.org/10.1016/j.geomorph.2009.05.003

Finsinger, W., Schwörer, C., Heiri, O., et al., 2019. Fire on ice and frozen trees? Inappropriate radiocarbon dating leads to unrealistic reconstructions. New Phytol. 222, 657–662. https://doi.org/10.1111/nph.15354

Gianotti, F., Forno, M.G., Ivy-Ochs, S., et al., 2015. Stratigraphy of the Ivrea morainic amphitheatre (NW Italy) an updated synthesis. Alp. Medit. Quat. 28, 29–58. ISSN: 2279-733

556 Goodfellow, B., 2007. Relict non-glacial surfaces in formerly glaciated landscapes. Earth-Sci. Rev.
557 80, 47–73. https://doi.org/10.1016/j.earscirev.2006.08.002
558 Grämiger, L.M., Moore, J.R., Gischig, V.S., et al., 2018. Thermomechanical stresses drive damage
559 of Alpine valley rock walls during repeat glacial cycles. J. Geophys. Res.: Earth Surface
560 123(10), 2620–2646. https://doi.org/10.1029/2018JF004626
561 Graven, H.D., 2015. Impact of fossil fuel emissions on atmospheric radiocarbon and various
562 applications of radiocarbon over this century. Proc. Nat. Academy Sci. 112(31), 9542–9545.
563 https://doi.org/10.1073/pnas.1504467112
564 Grove, J.M., 1988. The Little Ice Age. Methuen, London, pp. 498.
565 Gugerli, F., Holderegger, R., 2001. Nunatak survival, tabula rasa and the influence of the Pleistocene
566 ice-ages on plant evolution in mountain areas. Trends in Plant Science 6, 397–398.
567 https://doi.org/10.1016/S1360-1385(01)02053-2
568 Hampe, A., Rodríguez-Sánchez, F., Dobrowski, S., et al., 2013. Climate refugia: from the Last Glacial
569 Maximum to the twenty-first century. New Phytol. 197, 16–18.
570 https://doi.org/10.1111/nph.12059
571 Hatté, C., Pessenda, L.C., Lang, A., et al., 2001. Development of accurate and reliable ^{14}C
572 chronologies for loess deposits: application to the loess sequence of Nussloch (Rhine valley,
573 Germany). Radiocarbon 43(2B), 611–618. https://doi.org/10.1017/S0033822200041266
574 Hättestrand, C., Stroeven, A.P., 2002. A relict landscape in the centre of Fennoscandian glaciation;
575 geomorphological evidence of minimal Quaternary glacial erosion. Geomorphology 44(1–2),
576 127–143. https://doi.org/10.1016/S0169-555X(01)00149-0
577 Heiri, O., Koinig, K. A., Spötl, C., Barrett, S., Brauer, A., Drescher-Schneider, R., et al., 2014.
578 Palaeoclimate records 60–8 ka in the Austrian and Swiss Alps and their forelands. Quaternary
579 Science Reviews, 106, 186-205.https://doi.org/10.1016/j.quascirev.2014.05.021

Heiri, O., Ilyashuk, B., Millet, L., et al., 2015. Stacking of discontinuous regional palaeoclimate records: Chironomid-based summer temperatures from the Alpine region. The Holocene 25, 137–149. https://doi.org/10.1177/0959683614556382

Heiri, O., Millet, L., 2005. Reconstruction of Late Glacial summer temperatures from chironomid assemblages in Lac Lautrey (Jura, France). J. Quat. Sci. 20, 33–44. https://doi.org/10.1002/jqs.895

Hoffmann, H.M, 2016. Micro radiocarbon dating of the particulate organic carbon fraction in Alpine glacier ice: method refinement, critical evaluation and dating applications [PhD dissertation]. Combined Faculties for the Natural Sciences and for Mathematics of the Ruperto-Carola University of Heidelberg. https://doi.org/10.11588/heidok.00020712

Hormes, A., Karlén, W., Possnert, G., 2004. Radiocarbon dating of palaeosol components in moraines in Lapland, northern Sweden. Quat. Sci. Rev. 23(18-19), 2031–2043. https://doi.org/10.1016/j.quascirev.2004.02.004

Huber, K., Weckström, K., Drescher-Schneider, R., et al., 2010. Climate changes during the last glacial termination inferred from diatom-based temperatures and pollen in a sediment core from Längsee (Austria). J. Paleolimnol. 43, 131–147. https://doi.org/10.1007/s10933-009-9322-y

Ilyashuk, B.P., Gobet, E., Heiri, O., et al., 2009. Lateglacial environmental and climatic changes at the Maloja Pass, Central Swiss Alps, as recorded by chironomids and pollen. Quaternary Science Reviews 28(13-14), 1340–1353. https://doi.org/10.1016/j.quascirev.2009.01.007

IUSS Working Group WRB, 2015. World Reference Base for Soil Resources 2014, update 2015. International soil classification system for naming soils and creating legends for soil maps. World Soil Resources, Reports No. 106, FAO, Rome. E-ISBN 978-92-5-108370-3

Ivy-Ochs, S., 2015. Glacier variations in the European Alps at the end of the last glaciation. Cuadernos de Investigación Geográfica 41, 295. https://doi.org/10.18172/cig.2750

Ivy-Ochs, S., Kerschner, H., Reuther, A., et al., 2006a. The timing of glacier advances in the northern European Alps based on surface exposure dating with cosmogenic ^{10}Be, ^{26}Al, ^{36}Cl, and ^{21}Ne,

606 in: In Situ-Produced Cosmogenic Nuclides and Quantification of Geological Processes.
607 Geological Society of America. https://doi.org/10.1130/2006.2415(04)
608 Ivy-Ochs, S., Kerschner, H., Kubik, P.W., et al., 2006b. Glacier response in the European Alps to
609 Heinrich Event 1 cooling: the Gschnitz stadial. J. Quat. Sci. 21, 115–130.
610 https://doi.org/10.1002/jqs.955
611 Ivy-Ochs, S., Kerschner, H., Reuther, A., et al., 2008. Chronology of the last glacial cycle in the
612 European Alps. J. Quat. Sci. 23, 559–573. https://doi.org/10.1002/jqs.1202
613 Ivy-Ochs, S., Kerschner, H., Maisch, M., et al., 2009. Latest Pleistocene and Holocene glacier
614 variations in the European Alps. Quat. Sci. Rev. 28, 2137–2149.
615 https://doi.org/10.1016/j.quascirev.2009.03.009
616 Ivy-Ochs, S., Kober, F., 2013. COSMOGENIC NUCLIDE DATING | Exposure Geochronology, in:
617 Encyclopedia of Quaternary Science. Elsevier, 432–439. https://doi.org/10.1016/B978-0-444-
618 53643-3.00034-0
619 Jenk, T.M., Szidat, S., Bolius, D., et al., 2009. A novel radiocarbon dating technique applied to an ice
620 core from the Alps indicating late Pleistocene ages. J. Geophys. Res. 114, D14305.
621 https://doi.org/10.1029/2009JD011860
622 Jenk, T.M., Szidat, S., Schwikowski, M., et al., 2006. Radiocarbon analysis in an Alpine ice core:
623 record of anthropogenic and biogenic contributions to carbonaceous aerosols in the past (1650-
624 1940). Atmos. Chem. Phys. 6, 5381–5390. https://doi.org/10.5194/acp-6-5381-2006
625 Jost-Stauffer, M., Coope, G.R., Schlüchter, C., 2001. A coleopteran fauna from the middle Würm
626 (Weichselian) of Switzerland and its bearing on palaeobiogeography, palaeoeclimate and
627 palaeoecology. J. Quat. Sci. 16, 257–268. https://doi.org/10.1002/jqs.616
628 Karte, J., 1983. Periglacial Phenomena and their Significance as Climatic and Edaphic Indicators.
629 GeoJournal 7, 329–340.

630 Kelly, M.A., Buoncristiani, J.-F., Schlochter, C., 2004. A reconstruction of the last glacial maximum
631 (LGM) ice-surface geometry in the western Swiss Alps and contiguous Alpine regions in Italy
632 and France. Eclogae Geol. Helv. 97, 57–75. https://doi.org/10.1007/s00015-004-1109-6
633 Kerschner, H., Ivy-Ochs, S., Schlüchter, C., 2002. Die Moräne von Trins im Gschnitztal. Innsbrucker
634 Geographische Studien 33(2), 185–194.
635 Kerschner, H., Ivy-Ochs, S., 2008. Palaeoclimate from glaciers: Examples from the Eastern Alps
636 during the Alpine Lateglacial and early Holocene. Global Planet. Change 60, 58–71.
637 https://doi.org/10.1016/j.gloplacha.2006.07.034
638 Kerschner, H., Kaser, G., Sailer, R., 2000. Alpine Younger Dryas glaciers as palaeo-precipitation
639 gauges. Ann. Glaciol. 31, 80–84. https://doi.org/10.3189/172756400781820237
640 Kleman, J., Borgström, I., 1990. The boulder fields of Mt. Fulufjället, west-central Sweden.
641 Geografiska Annaler 72A (1), 63–78.
642 https://doiorg.bibliopass.unito.it/10.1080/04353676.1990.11880301
643 Köhler, P., 2016. Using the Suess effect on the stable carbon isotope to distinguish the future from
644 the past in radiocarbon. Environ. Res. Lett. 11(12), 124016.
645 https://iopscience.iop.org/article/10.1088/1748-9326/11/12/124016
646 Körner, C., 2003. Alpine Plant Life. Springer Berlin Heidelberg, Berlin, Heidelberg.
647 https://doi.org/10.1007/978-3-642-18970-8
648 Körner, C., Farquhar, G.D., Wong, S.C., 1991. Carbon isotope discrimination by plants follows
649 latitudinal and altitudinal trends. Oecologia 88(1), 30–40.
650 https://doiorg.bibliopass.unito.it/10.1007/BF00328400
651 Körner, C., Leuzinger, S., Riedl, S., et al., 2016. Carbon and nitrogen stable isotope signals for an
652 entire alpine flora, based on herbarium samples. Alp. Bot. 126(2), 153–166.
653 https://doi.org/10.1007/s00035-016-0170-x

654 Kosiński, P., Sękiewicz, K., Walas, Ł., et al., 2019. Spatial genetic structure of the endemic alpine
655 plant Salix serpillifolia: genetic swamping on nunataks due to secondary colonization? Alp.
656 Bot. 129(2), 107–121. https://doi-org.bibliopass.unito.it/10.1007/s00035-019-00224-4
657 Lang, G., 1994. Quartäre Vegetationsgeschichte Europas: Methoden und Ergebnisse. G. Fischer,
658 Schaffhausen.
659 Larocque-Tobler, I., Heiri, O., Wehrli, M., 2010. Late Glacial and Holocene temperature changes at
660 Egelsee, Switzerland, reconstructed using subfossil chironomids. J. Paleolimnol. 43, 649–666.
661 https://doi.org/10.1007/s10933-009-9358-z
662
663 Lowe, J.J., Walker, M.J., 2000. Radiocarbon Dating the Last Glacial-Interglacial Transition (Ca. 14–
664 9 ^{14}C Ka Bp) in Terrestrial and Marine Records: The Need for New Quality Assurance
665 Protocols 1. Radiocarbon 42(1), 53–68. https://doi.org/10.1017/S0033822200053054
666 Martinetto, E., 2009. Palaeoenvironmental significance of plant macrofossils from the Pianico
667 Formation, middle Pleistocene of Lombardy, north Italy. Quat. Int. 204(1-2), 20–30.
668 https://doi.org/10.1016/j.quaint.2008.11.014
669 Martinetto, E., Vassio, E., 2010. Reconstructing “Plant Community Scenarios” by means of
670 palaeocarpological data from the CENOFITA database, with an example from the Ca' Viettone
671 site (Pliocene, Northern Italy). Quat. Int. 225(1), 25–36.
672 https://doi.org/10.1016/j.quaint.2009.08.020
673 McCarroll, D., Ballantyne, C.K., Nesje, A., et al., 1995. Nunataks of the last ice sheet in northwest
674 Scotland. Boreas 24, 305–323. https://doi.org/10.1111/j.1502-3885.1995.tb00782.x
675 Mercalli, L., 2004. Il clima terrestre negli ultimi 10’000 anni. https://doi.org/10.5169/seals-132929
676 Monegato, G., Ravazzi, C., Donegana, M., et al., 2007. Evidence of a two-fold glacial advance during
677 the last glacial maximum in the Tagliamento end moraine system (eastern Alps). Quat. Res. 68,
678 284–302. https://doi.org/10.1016/j.yqres.2007.07.002

679 Monegato, G., Scardia, G., Hajdas, I., Rizzini, F., and Piccin, A., 2017. The Alpine LGM in the boreal
680 ice-sheets game. Scientific Reports, 7(1), 1-8. https://doi.org/10.1038/s41598-017-02148-7
681 Muhs, D.R., Ager, T.A., Bettis, E.A., et al., 2003. Stratigraphy and palaeoclimatic significance of
682 Late Quaternary loess-palaeosol sequences of the Last Interglacial-Glacial cycle in central
683 Alaska. Quat Sci Rev, 22(18–19): 1947–1986. https://doi.org/10.1016/S0277-3791(03)00167-
684 7
685 Nesje, A., Dahl, S.O., Anda, E., et al., 1988. Block fields in southern Norway: significance for the
686 Late Weichselian ice sheet. Norsk Geologisk Tidsskrift 68, 149–169.
687 Nesje, A., Dahl, S.O., 1993. Lateglacial and Holocene glacier fluctuations and clima te variations in
688 western Norway: a review. Quat. Sci. Rev. 12, 255–261. https://doi.org/10.1016/0277-
689 3791(93)90081-V
690 Orombelli, G., 1998. Le torbe del Rutor: una successione significativa per la storia olocenica dei
691 ghiacciai e del clima nelle Alpi. Memorie della Società Geografica Italiana 55, 153–165.
692 Orombelli, G., 2011. Holocene mountain glacier fluctuations: a global overview. Geografia Fisica e
693 Dinamica Quaternaria 34(1), 17–24.
694 Orombelli, G., Ravazzi, C., Cita, M.B., 2005. Osservazioni sul significato dei termini LGM (UMG),
695 Tardoglaciale e postglaciale in ambito globale, italiano ed alpino. Il Quaternario 18(2), 147–
696 156.
697 Paus, A., Velle, G., Larsen, J., et al., 2006. Lateglacial nunataks in central Scandinavia:
698 Biostratigraphical evidence for ice thickness from Lake Flåfattjønn, Tynset, Norway. Quat. Sci.
699 Rev. 25, 1228–1246. https://doi.org/10.1016/j.quascirev.2005.10.008
700 Pessenda, L. C., Gouveia, S. E., Aravena, R., 2001. Radiocarbon dating of total soil organic matter
701 and humin fraction and its comparison with ^{14}C ages of fossil charcoal. Radiocarbon 43(2B),
702 595–601.https://doi.org/10.1017/S0033822200041242
703 Peyron, O., Guiot, J., Cheddadi, R., et al., 1998. Climatic reconstruction in Europe for 18,000 yr BP
704 from pollen data. Quat. Res. 49, 183–196. https://doi.org/10.1006/qres.1997.1961

Pintaldi, E., D'Amico, M.E., Colombo, N., et al., 2021. Hidden soils and their carbon stocks at high-elevation in the European Alps (North-West Italy). Catena 198, 105044. https://doi.org/10.1016/j.catena.2020.105044

Pintaldi, E., D'Amico, M.E., Siniscalco, C., et al., 2016. Hummocks affect soil properties and soil-vegetation relationships in a subalpine grassland (North-Western Italian Alps). Catena 145, 214–226. https://doi.org/10.1016/j.catena.2016.06.014

Rasmussen, S.O., Andersen, K.K., Svensson, A.M., et al., 2006. A new Greenland ice core chronology for the last glacial termination. J. Geophys. Res. 111, D06102.

Ravazzi, C, 2005. Il Tardoglaciale: suddivisione stratigrafica, evoluzione sedimentaria e vegetazionale nelle Alpi e in Pianura Padana. Studi Trent. Sci. Nat., Acta Geol 82, 17–29.

Reitner, J.M., 2007. Glacial dynamics at the beginning of Termination I in the Eastern Alps and their stratigraphic implications. Quat. Int. 164–165, 64–84. https://doi.org/10.1016/j.quaint.2006.12.016

Renssen, H, Isarin, R.F.B., 2001. The two major warming phases of the last deglaciation at 14.7 and 11.5 ka cal BP in Europe: climatereconstructions and AGCM experiments. Global and Planetary Change 30, 117–153.

Renssen, H., Seppä, H., Heiri, O., et al., 2009. The spatial and temporal complexity of the Holocene thermal maximum. Nature Geoscience, 2(6), 411-414. https://doi.org/10.1038/ngeo513

Ruellan, A., 1971. The history of soils: some problems of definition and interpretation. In: Yaalon, D.H. (Ed.), PaleopedologydOrigin, Nature and Dating of Paleosols. International Society of Soil Science and Israel Universities Press, Jerusalem, Israel, pp. 3–13.

Rumpel, C., Kögel-Knabner, I., Bruhn, F., 2002. Vertical distribution, age and chemical composition of organic carbon in two forest soils of different pedogenesis. Org. Geochem. 3, 1131–1142. https://doi.org/10.1016/S0146-6380(02)00088-8

729 Samartin, S., Heiri, O., Lotter, A. F., et al., 2012a. Climate warming and vegetation response after
730 Heinrich event 1 (16 700–16 000 cal yr BP) in Europe south of the Alps. Climate of the Past
731 8(6), 1913–1927. https://doi.org/10.5194/cp-8-1913-2012
732 Samartin, S., Heiri, O., Vescovi, E., et al., 2012b. Lateglacial and early Holocene summer
733 temperatures in the southern Swiss Alps reconstructed using fossil chironomids. J. Quat. Sci.
734 27, 279–289. https://doi.org/10.1002/jqs.1542
735 Sartori, G., Mancabelli, A., Corradini, F., et al., 2001. Verso un catalogo dei suoli del Trentino: 3.
736 Rendzina (Rendzic Leptosols) e suoli rendziniformi. Studi Trentini Sci. Nat. Acta Geol. 76, 43–
737 70.
738 Scharpenseel, H.W., Becker-Heidmann, P., 1992. Twenty-five years of radiocarbon dating soils:
739 paradigm of erring and learning. Radiocarbon 34, 541–549. doi:10.1017/S0033822200063803
740 Scherrer, D., Koerner, C., 2010. Infra-red thermometry of alpine landscapes challenges climatic
741 warming projections. Global Change Biology 16(9), 2602–2613. https://doi-
742 org.bibliopass.unito.it/10.1111/j.1365-2486.2009.02122.x
743 Schmidt, R., Wunsam, S., Brosch, U., et al., 1998. Late and post-glacial history of meromictic
744 Längsee (Austria), in respect to climate change and anthropogenic impact. Aquat. Sci. 60, 56–
745 88
746 Schmidt, R., Weckström, K., Lauterbach, S., et al., 2012. North Atlantic climate impact on early late-
747 glacial climate oscillations in the south-eastern Alps inferred from a multi-proxy lake sediment
748 record. J. Quat. Sci. 27, 40–50. https://doi.org/10.1002/jqs.1505
749 Schönswetter, P., Stehlik, I., Holderegger, R., et al., 2005. Molecular evidence for glacial refugia of
750 mountain plants in the European Alps. Mol. Ecol. 14, 3547–3555.
751 https://doi.org/10.1111/j.1365-294X.2005.02683.x
752 Serra, E., Valla, P.G., Gribenski, N., et al., 2021. Geomorphic response to the Lateglacial–Holocene
753 transition in high Alpine regions (Sanetsch Pass, Swiss Alps). Boreas 50(1), 242–261.
754 https://doi-org.bibliopass.unito.it/10.1111/bor.12480

Smalley, I.J., Mavlyanova, N.G., Rakhmatullaev, K.L., et al., 2006. The formation of loess deposits in the Tashkent region and parts of Central Asia; and problems with irrigation, hydrocollapse and soil erosion. Quat. Int. 152, 59–69. https://doi.org/10.1016/j.quaint.2005.12.002

Stehlik, I., Blattner, F.R., Holderegger, R., et al., 2002. Nunatak survival of the high Alpine plant Eritrichium nanum (L.) Gaudin in the central Alps during the ice ages. Mol. Ecol. 11, 2027–2036. https://doi.org/10.1046/j.1365-294X.2002.01595.x

Stewart, J. R., Lister, A. M., 2001. Cryptic northern refugia and the origins of the modern biota. Trends in Ecology & Evolution 16(11), 608–613. https://doi.org/10.1016/S0169-5347(01)02338-2

Suess, H., 1955. Radiocarbon Concentration in Modern Wood. Science 122(3166), 415–417. http://www.jstor.org/stable/1751568

Ter Heerdt, G.N.J., Verweij, G.L., Bekker, R.M., et al., 1996. An improved method for seed-bank analysis: seedling emergence after removing the soil by sieving. Funct. Ecol. 10, 144–151. https://www.jstor.org/stable/2390273

Thevenon, F., Anselmetti, F.S., Bernasconi, S.M., et al., 2009. Mineral dust and elemental black carbon records from an Alpine ice core (Colle Gnifetti glacier) over the last millennium. J. Geophys. Res. 114, D17102. https://doi.org/10.1029/2008JD011490

Thorn, C.E., Darmody, R.G., Holmqvist, J., et al., 2009. Comparison of radiocarbon dating of buried paleosols using arbuscular mycorrhizae spores and bulk soil samples. The Holocene, 19(7), 1031-1037. https://doi-org.bibliopass.unito.it/10.1177/0959683609340997

Tinner, W., Kaltenrieder, P., 2005. Rapid responses of high-mountain vegetation to early Holocene environmental changes in the Swiss Alps. J. Ecol. 93(5), 936–947. https://www.jstor.org/stable/3599520

Tognetto, F., Perotti, L., Viani, C., et al., 2021. Geomorphology and geosystem services of the Indren-Cimalegna area (Monte Rosa massif – Western Italian Alps). Journal of Maps 17(2), 161–172. DOI:10.1080/17445647.2021.1898484

781 Tonneijck, F.H., van der Plicht, J., Jansen, B., et al., 2006. Radiocarbon dating of soil organic matter
782 fractions in Andosols in northern Ecuador. Radiocarbon 48(3), 337–353.
783 https://doi.org/10.1017/S0033822200038790
784 van Vliet-Lanoë, B. 1998. Pattern ground, hummocks, and Holocene climatic changes. Eurasian Soil
785 Sci. 31, 507–513.
786 Vescovi, E., Ravazzi, C., Arpenti, E., et al., 2007. Interactions between climate and vegetation during
787 the Lateglacial period as recorded by lake and mire sediment archives in Northern Italy and
788 Southern Switzerland. Quat. Sci. Rev. 26, 1650–1669.
789 https://doi.org/10.1016/j.quascirev.2007.03.005
790 Wagenbach, D., Geis, K., 1989. The mineral dust record in a high altitude Alpine glacier (Colle
791 Gnifetti, Swiss Alps). In Paleoclimatology and paleometeorology: modern and past patterns of
792 global atmospheric transport (pp. 543-564). Springer, Dordrecht.
793 Wagenbach D., Preunkert S., Schäfer J., et al., 1996. Northward Transport of Saharan Dust Recorded
794 in a Deep Alpine Ice Core. In: Guerzoni S., Chester R. (eds) The Impact of Desert Dust Across
795 the Mediterranean. Environmental Science and Technology Library, vol 11. Springer,
796 Dordrecht.
797 Walker, M.J., Björck, S., Lowe, J.J., et al., 1999. Isotopic ‘events’ in the GRIP ice core: a stratotype
798 for the Late Pleistocene. Quat. Sci. Rev. 18, 1143–1150.
799 Wang, Y., Amundson, R., Trumbore, S., 1996. Radiocarbon dating of soil organic matter. Quaternary
800 Research 45(3), 282–288. https://doi.org/10.1006/qres.1996.0029
801 Wang, Z., Zhao, H., Dong, G., et al., 2014. Reliability of radiocarbon dating on various fractions of
802 loess-soil sequence for Dadiwan section in the western Chinese Loess Plateau. Frontiers of
803 Earth Science 8(4), 540–546. DOI 10.1007/s11707-014-0431-1
804 Wilson, P., 2013. Block/rock streams. The Encyclopedia of Quaternary Science 3, 514–522.
805 https://doi.org/10.1016/B978-0-444-53643-3.00102-3

806 Wirsig, C., Zasadni, J., Christl, M., et al., 2016. Dating the onset of LGM ice surface lowering in the
807 High Alps. Quat. Sci. Rev. 143, 37–50. https://doi.org/10.1016/j.quascirev.2016.05.001
808

Figures

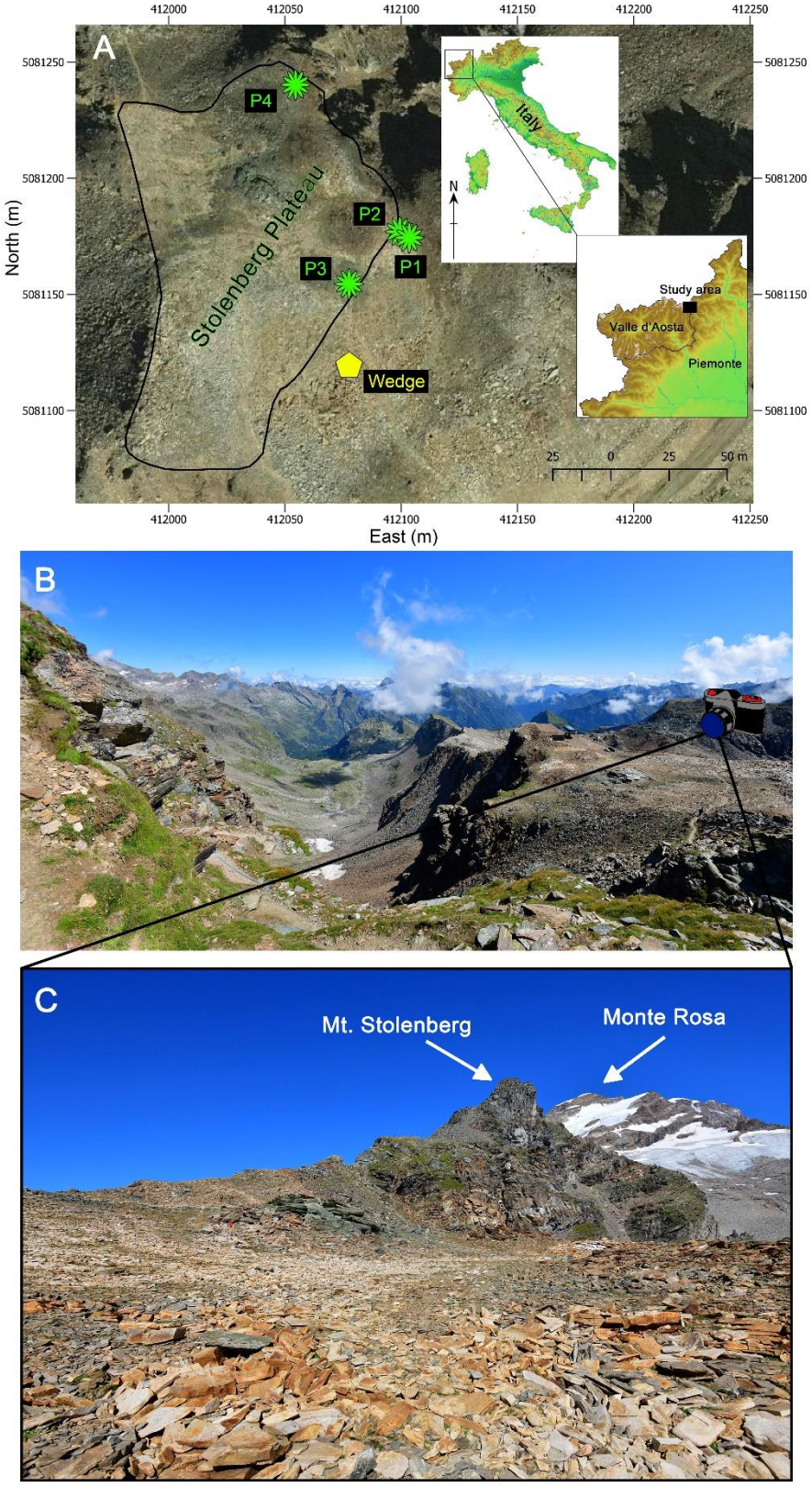

Figure 1. (a) Location of the study area in the NW Italian Alps (www.pcn.minambiente.it) and overview of the study area (orthoimage Piemonte Region, year 2010) (coordinate system WGS 84 / UTM zone 32N); green forms indicate the location of the three soil profiles (P1, P2, P3) and the vegetated patch (P4); yellow polygon indicates

the location of the soil-filled wedge. (b) View of the Plateau from the base of the Mt. Stolenberg (photo by M. D'Amico). (c) View of the Plateau (photo by M. D'Amico).

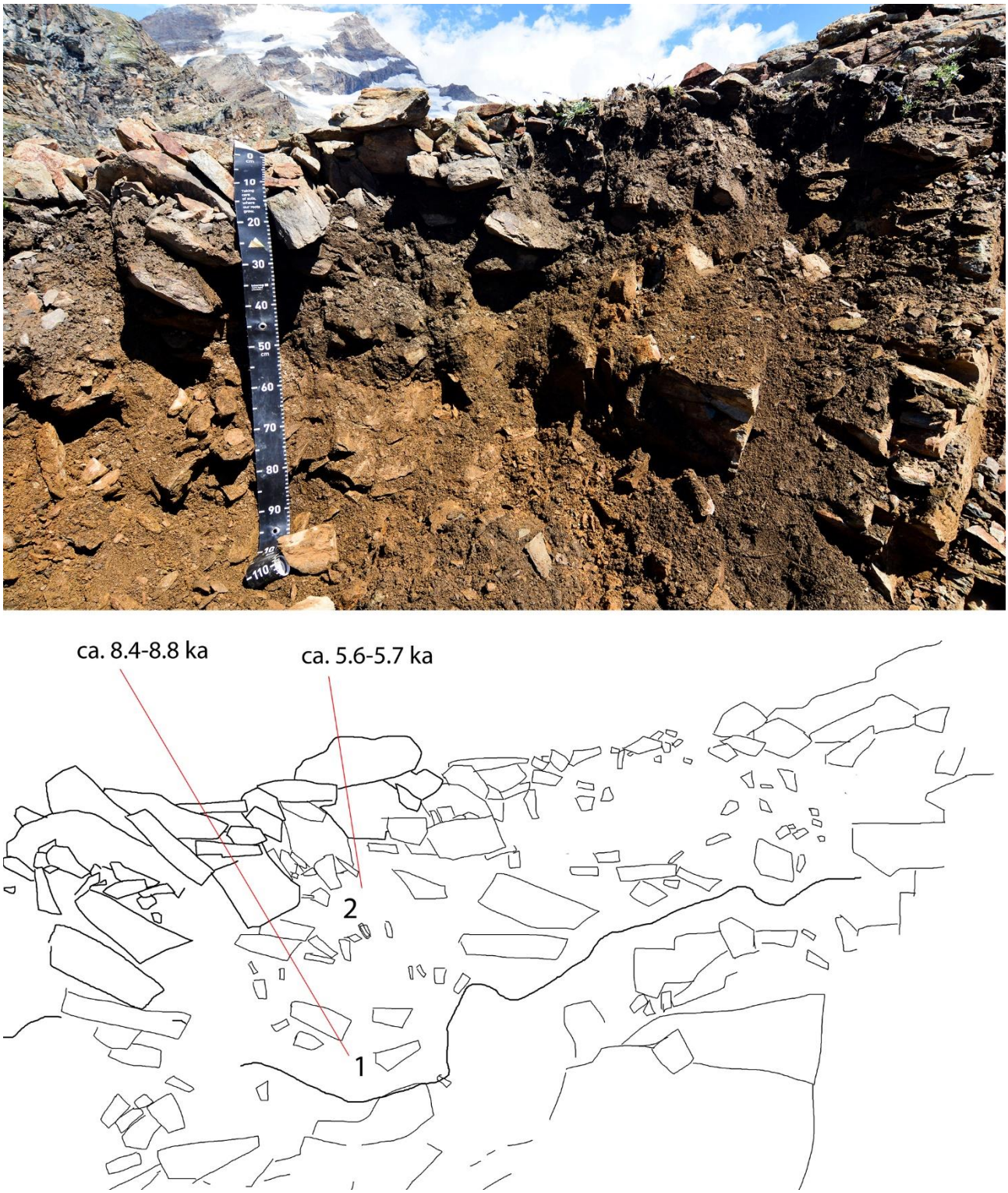

Figure 2. Soil profile P1, with the corresponding scheme (below) reporting sampling points (number), the horizon limits (lines therein), and the age of soil samples (ka cal. BP). P1-1 and P1-2 were analyzed for ^{14}C (Tab. 2) and $\delta^{13}C$ (Tab. 3).

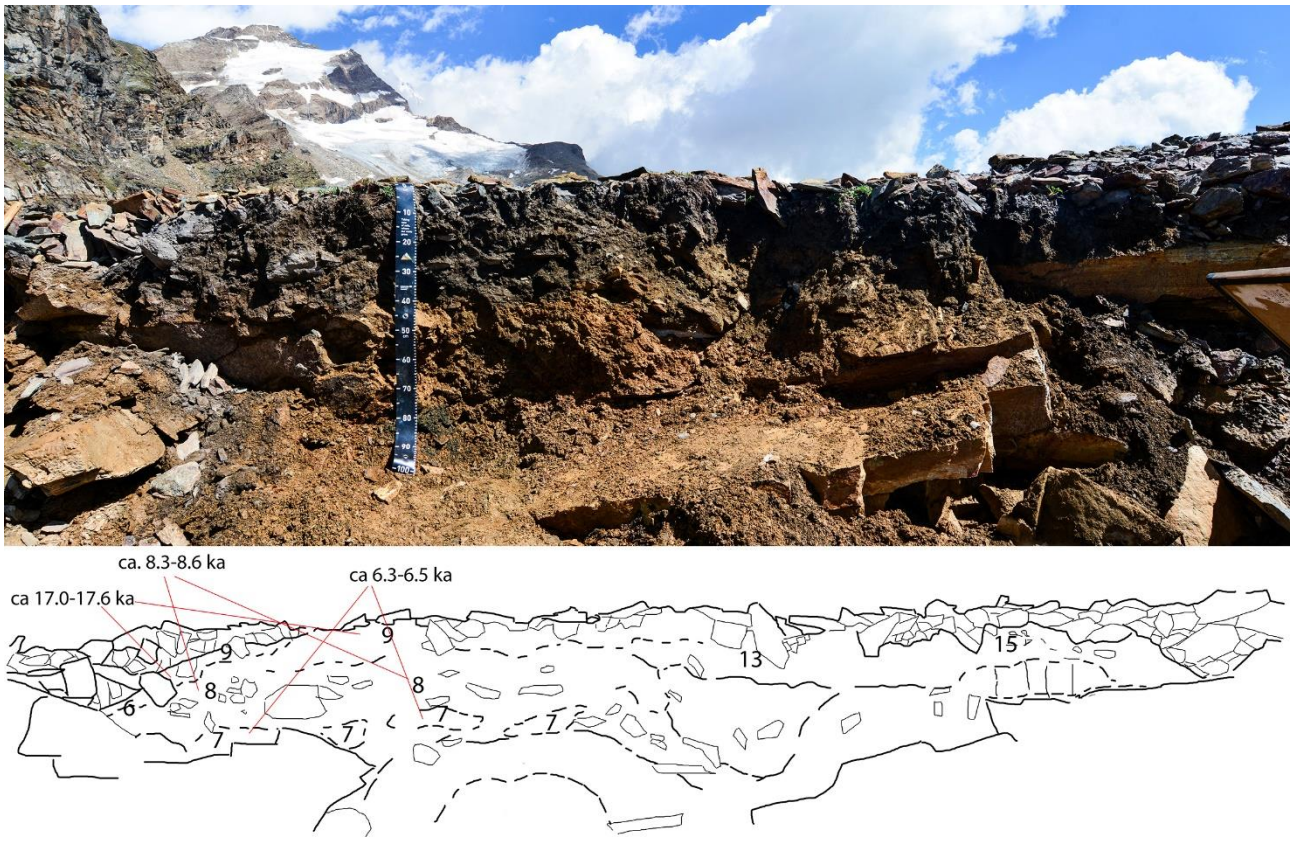

Figure 3. Soil profile P2, with the corresponding scheme (below) reporting sampling points (number), the horizon limits (lines therein), and the age of soil samples (cal. ka BP). P2-7, P2-8, and P2-9 (and P2-9bis, not shown in the figure) were analyzed for ^{14}C (Tab. 2); P2-7, P2-8, P2-9 (and P2-9bis), P2-13, and P2-15 were analyzed for $\delta^{13}C$ (Tab. 3).

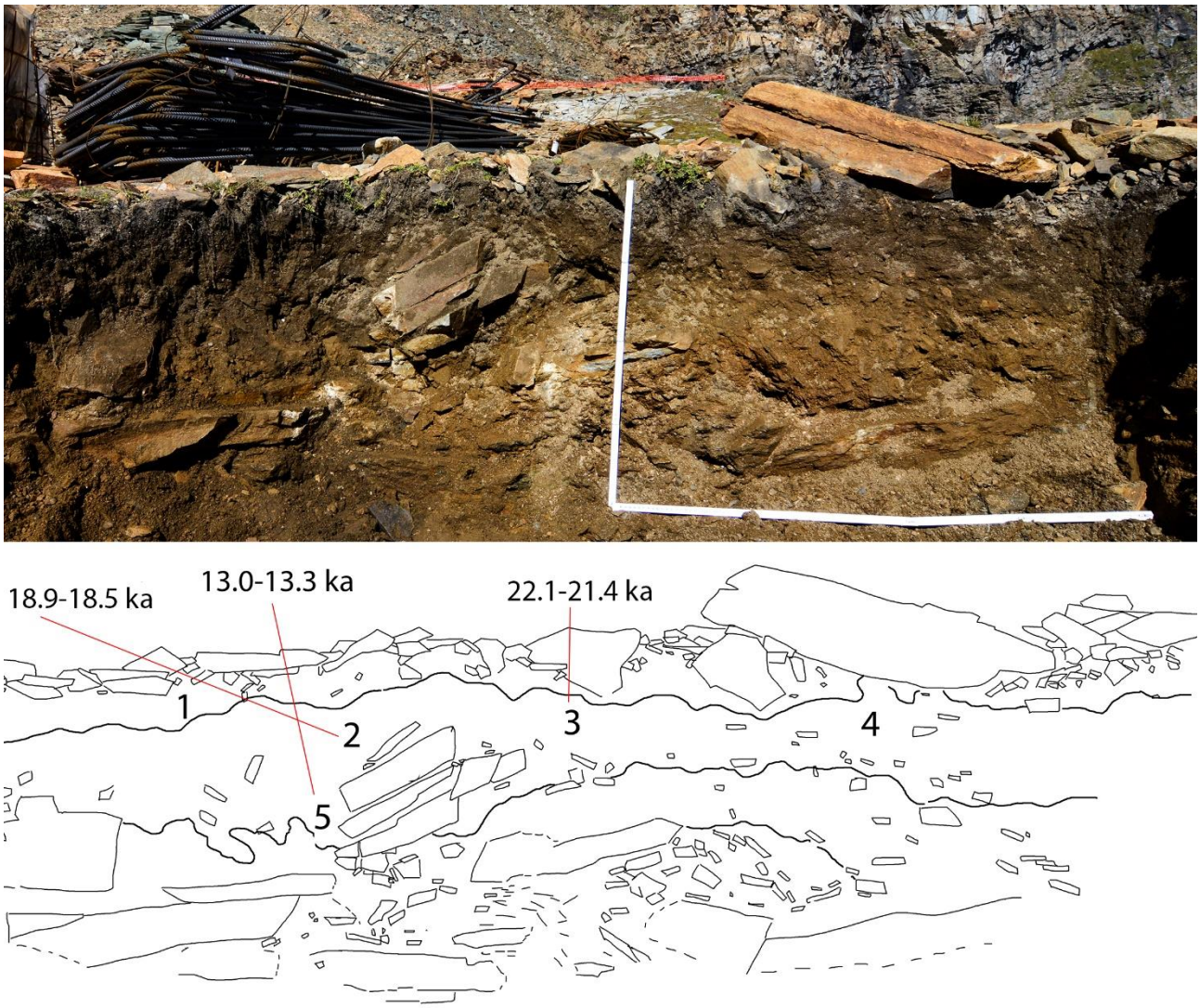

826
827 **Figure 4. Soil profile P3, with the corresponding scheme (below) reporting sampling points (number), the horizon**
828 **limits (lines therein), and the age of soil samples (ka cal. BP). P3-2, P3-3, and P3-5 were analyzed for ^{14}C (Tab. 2); P3-**
829 **1, P3-2, P3-3, P3-4, and P3-5 were analyzed for $\delta^{13}C$ (Tab. 3).**

830

831

832
833

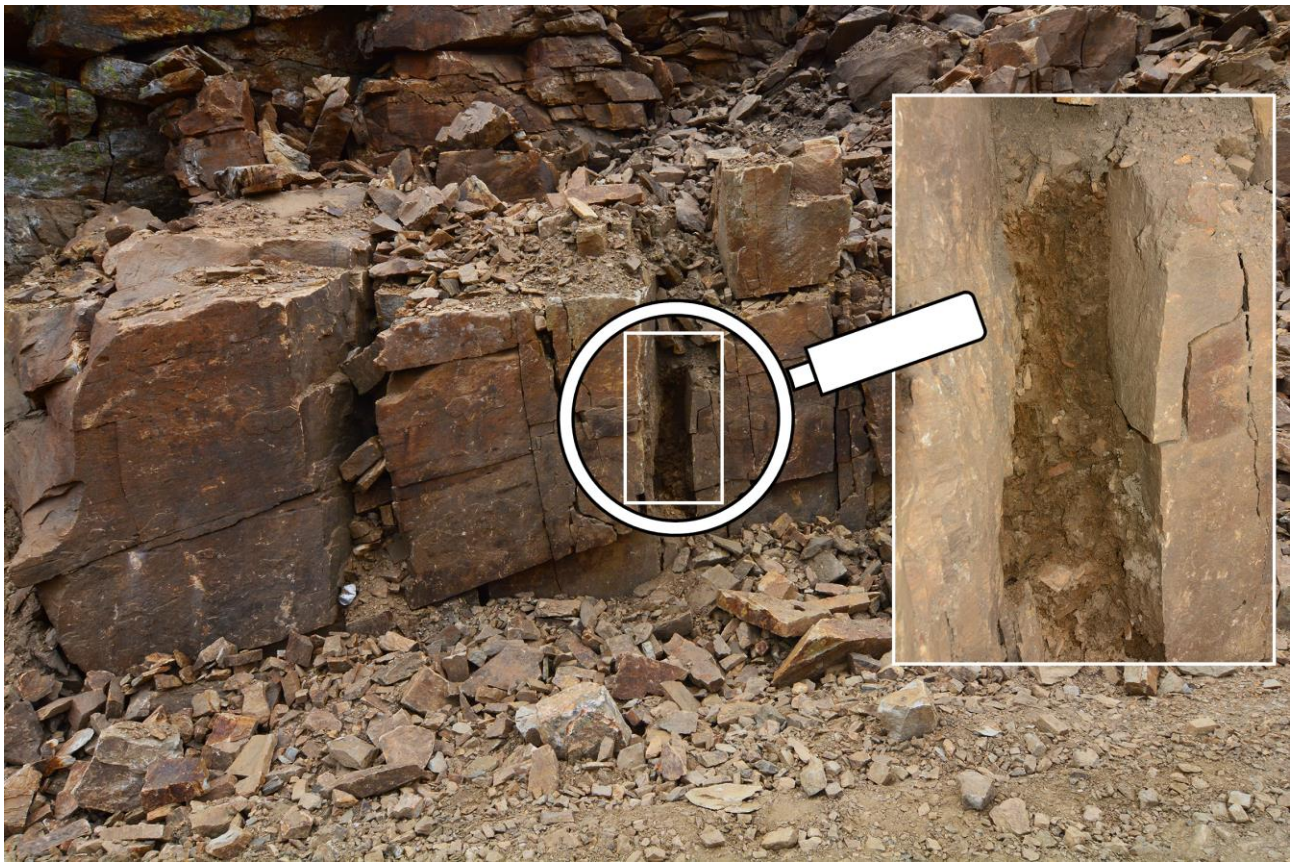

Figure 5. The soil-filled rock wedge along the southern border of the Plateau and detail of the sampling site.

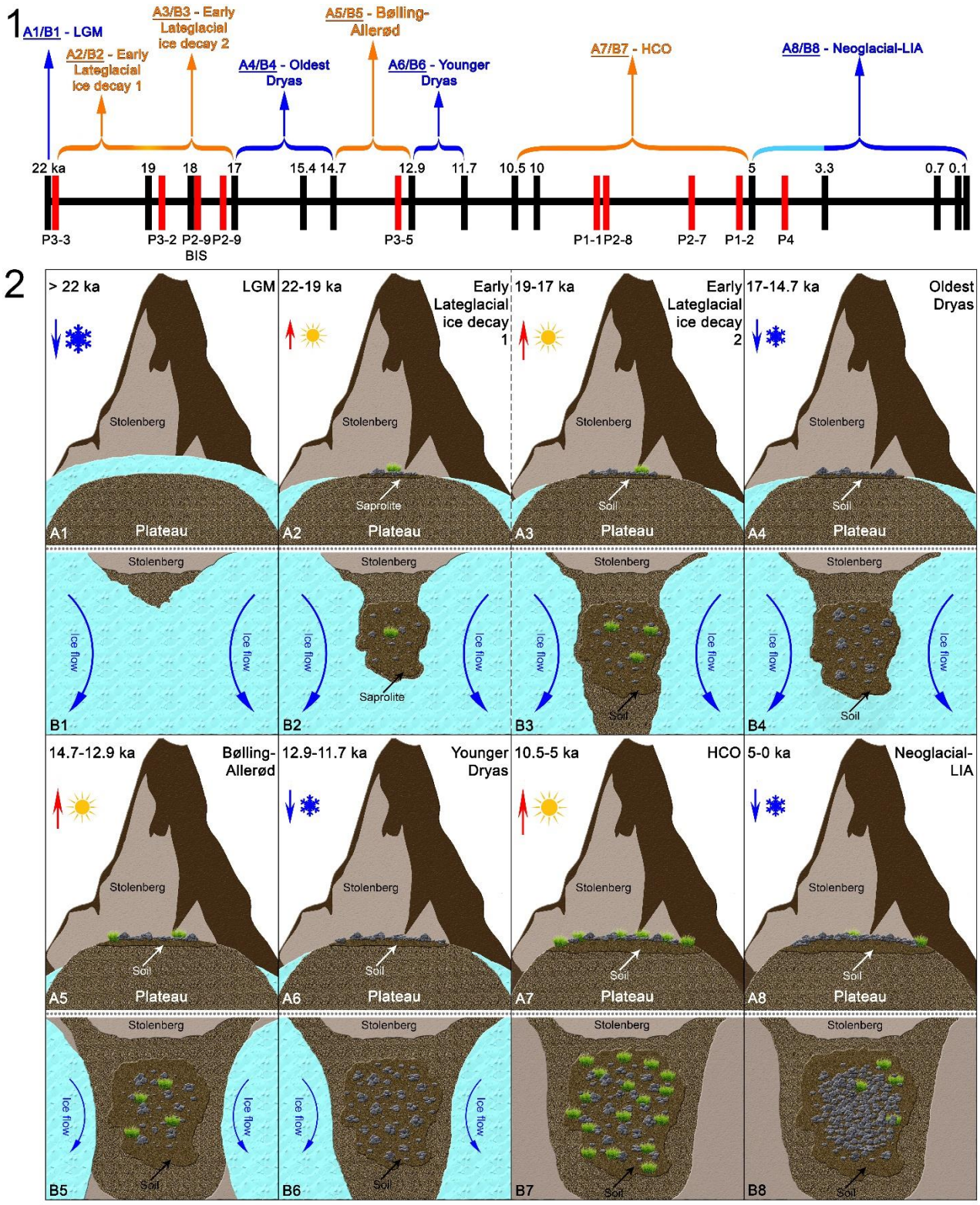

Figure 6. Tentative paleoenvironmental reconstruction of the Stolenberg Plateau based on the findings in this paper and on literature reported in the text. (1) Reference timeline from LGM to present day: blue colors indicate cooling phases, orange ones warming phases, the light blue segment (on the right) indicates a period of progressive cooling occurred at the beginning of Neoglacial phase; red segments indicate the age of soil samples reported in table 2. (2) Corresponding visual of the Plateau during the different phases: letters A (A1, A2, etc.) are the frontal views, B ones are the planimetric views. Details in the text.

Tables

Profile samples		
Family/Genus/Species	**N° (seeds/fruits/leaves)**	**Frequency (%)**
Asteraceae indet.	1	0.3
Brassicaceae indet.	1	0.3
Carex parviflora	1	0.3
Carex myosuroides	7	1.9
Cerastium sp.	16	4.4
Cerastium uniflorum	90	24.6
Cirsium sp.	1	0.3
Crepis sp.	1	0.3
Draba sp.	1	0.3
Gentiana gr. *verna*	1	0.3
Juncus sp.	1	0.3
Leucanthemopsis alpina	1	0.3
Minuartia sp.	23	6.3
Oxyria digyna	1	0.3
Poaceae sp.	75	20.5
Potentilla sp.	1	0.3
Salix cf. *herbacea*	103	28.1
Saxifraga oppositifolia	10	2.7
Sibbaldia procumbens	1	0.3
Silene acaulis	27	7.4
Taraxacum cf. *alpinum*	2	0.5
cf. *Vaccinium uliginosum*	1	0.3
TOT	366	100.0
Wedge sample (F)		
Family/Genus/Species	**N° (seeds/fruits/leaves)**	**Frequency (%)**
cf. *Artemisia*	1	5.9
Carex myosuroides	1	5.9
Cerastium sp.	1	5.9
Juncus sp.	1	5.9
Poaceae indet.	8	47.1
Primulaceae	1	5.9
Selaginella selaginoides	1	5.9
Silene acaulis	1	5.9
Taraxacum cf. *alpinum*	1	5.9
cf. *Vaccinium uliginosum*	1	5.9
TOT	17	100.0

Table 1. Results of the carpology investigation: identified plant taxa within soil samples collected from the Umbric horizons in the soil profiles and from the soil-filled rock wedge.

Lab. Code	Sample ID	TOC (g/kg)*	Type	Radiocarbon Age (yr BP)	Cal. Radiocarbon Age (yrs cal. BP) (confidence level 2σ)	Phase
LTL19173A	P1-1	19.0	Soil	7798 ± 75	8782-8412 (92.1%)	HCO
LTL19174A	P1-2	10.8	Soil	4918 ± 45	5735-5589 (95.4%)	HCO
LTL19175A	P2-7	20.5	Soil	5639 ± 45	6506-6306 (95.4%)	HCO
LTL19172A	P2-8	11.0	Soil	7608 ± 75	8561-8300 (92.1%)	HCO
LTL19176A	P2-9	11.3	Soil	14203 ± 100	17584-16985 (95.4%)	ELID
LTL19542A	P2-9bis	12.5	Soil	14745 ± 70	18148-17719 (95.4%)	ELID
LTL19169A	P3-2	8.7	Soil	15463 ± 100	18921-18518 (95.4%)	ELID
LTL19543A	P3-3	10.6	Soil	17978 ± 120	22145-21427 (95.4%)	LGM/ELID
LTL19170A	P3-5	11.8	Soil	11345 ± 65	13306-13076 (95.4%)	BA
LTL19871A	P4	13.8	Soil	3820 ± 45	4360-4090 (88.5%)	HCO-NG
LTL19865A	A	-	Plant	-	After 1950 AD	M
LTL19866A	B	-	Plant	-	After 1950 AD	M
LTL19867A	C	-	Plant	-	After 1950 AD	M
LTL19868A	D	-	Plant	-	After 1950 AD	M
LTL19869A	E	-	Plant	-	After 1950 AD	M
LTL19870A	F	-	Plant	1789 ± 45	1824-1594 (94.0%)	RWP

Table 2. Radiocarbon ^{14}C dating results of soil samples and plant fragments. HCO: Holocene Climatic Optimum; ELID: Early Lateglacial Ice Decay; BA: Bølling-Allerød; NG: Neoglacial; M: Modern; RWP: Roman Warm Period. *Total Organic Carbon (TOC) values derived from Pintaldi et al. (2021).

Site	Elevation (m a.s.l.)	Cover type	$\delta^{13}C$ (‰)
S1	2840	Vegetation	-23.3
S2	2800	Vegetation	-25.1
S3	2770	Vegetation	-25.7
S6	2854	Vegetation	-23.4
S8	2749	Vegetation	-23.4
P4	3030	Vegetation	-22.7
P1-1	3030	Blockstream/Blockfield	-24.7
P1-2	3030	Blockstream/Blockfield	-23.9
P2-7	3030	Blockstream/Blockfield	-24.2
P2-8	3030	Blockstream/Blockfield	-23.9
P2-9	3030	Blockstream/Blockfield	-24.5
P2-9bis	3030	Blockstream/Blockfield	-24.5
P2-13	3030	Blockstream/Blockfield	-24.0
P2-15	3030	Blockstream/Blockfield	-24.3
P3-1	3030	Blockstream/Blockfield	-24.6
P3-2	3030	Blockstream/Blockfield	-23.8
P3-3	3030	Blockstream/Blockfield	-23.5
P3-4	3030	Blockstream/Blockfield	-24.0
P3-5	3030	Blockstream/Blockfield	-23.6

858
859 **Table 3. IRMS $\delta^{13}C$ results of present-day vegetated soils in the study area and soils from the Plateau under blockstream/blockfield.**